A Fine-Grained Analysis of Millimeter-Wave Device-to-Device Networks

Na Deng and Martin Haenggi, *Fellow, IEEE*

***Abstract*—Enabling device-to-device (D2D) communications in millimeter-wave (mm-wave) networks is of critical importance for the next-generation mobile networks to support very high data rates (multi-gigabits-per-second) for mobile devices. In this paper, we provide a fine-grained performance analysis of the mm-wave D2D communication networks. Specifically, we first establish a general and tractable framework to investigate the performance of mm-wave D2D networks using the Poisson bipolar model integrated with several features of the mm-wave band. To show what fraction of users in the network achieve a target reliability if the required signal-to-interference-plus-noise ratio (SINR) (or QoS requirement) is given, we derive the meta distributions of the SINR and the data rate. Interestingly, in mm-wave D2D networks, the standard beta approximation for the meta distribution does not work very well when highly directional antenna arrays are used or the node density is small. To resolve this issue, we provide a modified approximation by using higher moments of the conditional SINR distribution, which is shown to be closer to the exact result. On this basis, we also derive the mean local delay and spatial outage capacity to provide a comprehensive investigation on the impact of mm-wave features on the performance of D2D communication.**

***Index Terms*—Stochastic geometry; Poisson point process; meta distribution; mean local delay; spatial outage capacity; millimeter wave; D2D communication.**

I. Introduction

A. Motivation

With the explosive growth of mobile devices and emerging applications, the tension between capacity requirements and spectrum shortage becomes increasingly prominent. To mitigate this dilemma, the two options are to exploit new spectrum resources or to increase the spectrum efficiency. Recently, the wireless industry has turned its attention to the millimeter wave (mm-wave) band, between 30 and 300 GHz, expecting to take advantage of the huge and unexploited bandwidth to cope with the future multi-gigabit-per-second data rate demand [2, 3]. Besides using new wireless spectrum, 5G systems will also exploit intelligence at the device side (e.g., by allowing device-to-device (D2D) connectivity) to provide higher spectrum efficiency, reduced end-to-end latency and increased throughput [3]. Generally, D2D connections can be set up between two devices either directly or by relaying with or without base station (BS) involvement. For existing communication systems, the main challenge of implementing underlaid D2D links is the difficulty in interference management between the intra-D2D interference and the cross-tier interference from other systems using the same spectrum, especially for the autonomous case without BS involvement [4]. However, since the mm-wave spectrum has several unique features such as spectrum availability, high propagation loss, directivity, and sensitivity to blockage, the situation will be different when the D2D communication occurs in the mm-wave band. For example, since the antenna dimension is inversely proportional to the frequency, the mm-wave D2D users equipped with very small and highly directional antennas cause much less interference than the D2D users adopting omni-directional antennas. Another important benefit is that the new spectrum facilitates the more wide-spread use of (autonomous) D2D communication. By operating in mm-wave band, there is no cross-tier interference between the D2D network and the sub-6 GHz cellular systems, especially for the autonomous type where the cross-tier interference is quite serious and hard to be controlled if both D2D and cellular transmissions occur in the same band. Accordingly, both the signaling overheads and the loads of BSs can be reduced significantly. Thus, mm-wave D2D communication is of critical importance for the next-generation mobile networks and deserves in-depth investigations on how to exploit the salient properties of mm-wave communication for D2D networks and to analyze their performance. This is the focus of our paper.

B. Related Work

Stochastic geometry has been successfully applied to model and analyze wireless networks in the last two decades since it not only captures the topological randomness in the network geometry but also leads to tractable analytical results [5–7]. Prior work on mm-wave based networks has mostly used the Poisson point process (PPP) to model the spatial distribution of nodes and analyzed coverage and rate while modeling the directionality of antennas and the effect of blockages [8–10]. For D2D-based networks, there also exists a growing body of literature using the PPP to model the irregular spatial structure of D2D users and base stations [11, 12]. Very recently, researchers have started to pay attention to the benefits of combining mm-wave and D2D technologies. Specifically, [13] studied the path loss behavior in urban environment for mm-wave D2D links based on a ray tracing simulation. [14] considered D2D connectivity in mm-wave networks, where

Na Deng is with the School of Information and Communication Engineering, Dalian University of Technology (DLUT), Dalian, 116024, China (e-mail: dengna@dlut.edu.cn). Martin Haenggi is with the Dept. of Electrical Engineering, University of Notre Dame, Notre Dame 46556, USA (e-mail: mhaenggi@nd.edu).

Part of this work is under submission at the 2017 IEEE Global Communications Conference (GLOBECOM' 17) [1].

This work was supported by the Fundamental Research Funds for the Central Universities (DUT16RC(3)119) and by the US NSF grant CCF 1525904.

the probability distribution, mean, and variance of the inter-device distance were derived, and the connectivity performances of both the direct and indirect D2D communications were investigated. [15] used stochastic geometry to analyze the performance of mm-wave D2D networks with a finite number of interferers in a finite network region. These works investigated the mm-wave D2D networks either through pure simulations or theoretical analysis with a finite spatial extent. Only [16] analyzed the downlink coverage probability of a D2D relay-assisted mm-wave cellular network where the obstacles, BSs, and users formed independent homogeneous PPPs.

The signal-to-interference-plus-noise ratio (SINR) is a fundamental metric to understand how a communication system/network performs. When stochastic geometry is used for the analysis, the SINR performance is most commonly characterized as the success probability relative to an SINR threshold and evaluated at the typical link. However, the performance of the typical link represents an average over all the spatial realizations of the point process (or over all the links in a single realization if the point process is ergodic), which provides very limited information on the individual links. To overcome this limitation, [17] introduced the concept of the *meta distribution*, which is the distribution of the conditional success probability given the point process. Conditioned on the PPP, the success probability of each individual link is calculated by averaging over the fading and the random activity of the interferers. The *distribution* of these conditional success probabilities, obtained by an expectation over the point process is the meta distribution. In contrast, the standard success probability is the *mean* of the conditional success probability. Consequently, the meta distribution provides a much sharper characterization of the network performance (i.e., the SINR performance). While [17] focused on the meta distribution of the signal-to-interference ratio (SIR) in both the Poisson bipolar networks with ALOHA channel access and the downlink of Poisson cellular networks, [18] and [19] applied the SIR meta distribution to study the D2D communication underlaying cellular networks and fractional power control for cellular networks in microwave bands, respectively. Different from them, we focus on the meta distributions of the SINR and the achievable rate in mm-wave D2D networks considering the unique channel characteristics and antenna features of mm-wave communications.

C. Contributions

The main objective of this paper is to introduce and promote the meta distribution as a key performance metric for mm-wave D2D networks. The desirable features of mm-wave, which include spectrum availability, small antenna dimensions enabling the implementation of highly directive antenna arrays, natural interference suppression, and dense deployability, motivate us to carry out a comprehensive investigation on the performance of the network by combining the two promising technologies, i.e., mm-wave and D2D, aiming at finding the most efficient way to operate D2D in mm-wave frequencies.

Specifically, we first give a closed-form expression for the moments of the conditional success probability for mm-wave D2D networks considering the effects of blockage and the large beamforming gain from directional antenna arrays. Next, to show what fraction of users in the network achieve a target reliability (or transmission effectiveness) if the SINR (or QoS) requirement is given, we provide analytical expressions for the exact meta distributions of the SINR and the data rate, which are the distributions of the conditional success probability and the conditional achievable rate given the point process, respectively. Due to the unique features of mm-wave, the standard beta distributed approximation proposed for microwave networks does not work very well when highly directional antenna arrays are used or the network node density is small. Thus, we propose a general beta distribution as a modified and more accurate approximation for the meta distribution. On this basis, the mean local delay and spatial outage capacity (SOC) (first introduced in [20]) are also calculated for mm-wave D2D links and networks, respectively. Finally, the impacts of mm-wave features, the link distance between D2D users, and the density of users on each performance metric are investigated numerically, which show that the unique features of the mm-wave band and the user density have significant effects on the interference (i.e., when the network is interference-limited and when it is not) and hence the performance of mm-wave D2D networks.

D. Organization

The rest of the paper is organized as follows: Section II introduces the system model with blockage effect and antenna pattern gain. Section III gives a general framework for a fine-grained analysis of mm-wave D2D networks, including the moments of the conditional success probability, the meta distributions of the SINR and the data rate, the mean local delay, and the spatial outage capacity. Section IV presents the numerical results, and Section V offers the concluding remarks.

II. System Model

A. Network Model

We consider a mm-wave D2D communication network, where the D2D transmitters are distributed according to a homogeneous PPP Φ with density λ. Each transmitter is assumed to have a dedicated receiver at distance r_0 in a random orientation, i.e., the D2D users form a *Poisson bipolar network* [7, Def. 5.8]. We consider a receiver at the origin that attempts to receive from an additional transmitter located at $(r_0, 0)$. Due to Slivnyak's theorem [7, Thm. 8.10], this receiver becomes the typical receiver under expectation over the PPP. We assume that each receiver has a single antenna and its corresponding transmitter is equipped with a square antenna array composed of N elements. All transmitters operate at a constant power μ and apply analog beamforming to overcome the severe path loss in the mm-wave band. We also assume that the direction of arrival (DoA) between the transmitter-receiver pair is known at the transmitter and thus the beam direction is perfectly aligned to obtain the maximum power gain. The ALOHA channel access scheme is adopted, i.e., in each time slot, D2D transmitters in Φ independently transmit with probability p.

TABLE I. Antenna parameters of a uniform planar square antenna array [16]

Parameters	Description	value
w	Half-power beamwidth	$\frac{\sqrt{3}}{\sqrt{N}}$
G_{m}	Main lobe gain	N
G_{s}	Side lobe gain	$1/\sin^2\left(\frac{3\pi}{2\sqrt{N}}\right)$

B. Blockage and Propagation Model

The generalized LOS ball model [21] is used to capture the blockage effect in mm-wave communication since it has been validated in [9] as a better fit with real-world scenarios than other blockage models adopted in previous works. Specifically, the LOS probability of the channel between two nodes with separation d in this model is

$$P_{\mathrm{LOS}}(d) = p_{\mathrm{L}}\mathbf{1}(d < R), \tag{1}$$

where $\mathbf{1}(\cdot)$ is the indicator function, R is the maximum length of a LOS channel, and the LOS fraction constant $p_{\mathrm{L}} \in [0,\ 1]$ represents the average fraction of the LOS area within a circular ball of radius R around the receiver under consideration. Thus, p_{L} is the LOS probability if the distance d is less than R. The blockage effect induces different path loss exponents, denoted as α_{L} and α_{N}, for LOS and NLOS channels, respectively. Typical values for mm-wave path loss exponents can be found in measurement results in [22] with approximated ranges of $\alpha_{\mathrm{L}} \in [1.9, 2.5]$ and $\alpha_{\mathrm{N}} \in [2.5, 4.7]$.

For the sake of mathematical tractability, the sectorized antenna model is adopted to approximate the actual antenna pattern, as in [21]. In particular, the array gains within the half-power beam width are assumed to be the maximum power gain (i.e., main lobe gain), and the gains of the other DoAs are approximated to be the first minor maximum gain (i.e., side lobe gain) of the actual antenna pattern, which can be formulated as

$$G(\varphi) = \begin{cases} G_{\mathrm{m}} & \text{if } |\varphi| \le w/2 \\ G_{\mathrm{s}} & \text{otherwise,} \end{cases} \tag{2}$$

where $w \in (0, 2\pi]$ is the half-power beam width and correlated with the size of antenna array, and $\varphi \in [-\pi, \pi)$ is the angle off the boresight direction. With the assumption of a $\sqrt{N} \times \sqrt{N}$ uniform planar square antenna array with half-wavelength antenna spacing, the half-power beamwidth w, main lobe gain G_{m}, and side lobe gain G_{s} are summarized in Table I.

C. SINR Analysis

We assume that the desired link between the transmitter-receiver pair is in the LOS condition with deterministic path loss $r_0^{-\alpha_{\mathrm{L}}}$. In fact, if the receiver was associated with a NLOS transmitter, the link would quite likely be in outage due to the severe propagation loss and high noise power at mm-wave bands as well as the fact that the interferers can be arbitrarily close to the receiver. The power fading coefficient associated with node $x \in \Phi$ is denoted by h_x, which is an exponential random variable with $\mathbb{E}(h_x) = 1$ (Rayleigh fading[1]) for both LOS and NLOS to enhance the analytical tractability, and all h_x are mutually independent and also independent of the point process Φ. $\ell(x)$ is the random path loss function[2] associated with the interfering transmitter location x, given by

$$\ell(x) = \begin{cases} |x|^{-\alpha_{\mathrm{L}}} & \text{w.p. } P_{\mathrm{LOS}}(|x|) \\ |x|^{-\alpha_{\mathrm{N}}} & \text{w.p. } 1 - P_{\mathrm{LOS}}(|x|), \end{cases} \tag{3}$$

where all $\ell(x)_{x\in\Phi}$ are independent. For the typical receiver, the interferers outside the LOS ball are NLOS and thus can be ignored due to the severe path loss over the large distance (at least R). As a result, the analysis for the network originally composed by the PPP Φ with density λ reduces to the analysis of a finite network region, namely the disk of radius R centered at the origin. Due to the incorporation of the blockages, the LOS transmitters with LOS propagation to the typical receiver form a PPP Φ_{L} with density $p_{\mathrm{L}}\lambda$, while Φ_{N} with density $p_{\mathrm{N}}\lambda$ is the transmitter set with NLOS propagation, where $p_{\mathrm{L}}+p_{\mathrm{N}} = 1$ such that $\Phi = \Phi_{\mathrm{L}} \cup \Phi_{\mathrm{N}}$.

Thus, the interference at the origin is defined as

$$I \triangleq \sum_{x\in\Phi} \mu G(\varphi_x) h_x \ell(x) B_x, \tag{4}$$

where μ is the constant transmit power, $G(\varphi_x)$ is the directional antenna gain function with DoA φ_x, and B_x is a Bernoulli variable with parameter p to indicate whether x transmits a message to its receiver. Since all transmitters are oriented toward the corresponding receivers, the DoAs between the interferers and the typical receiver are uniformly random in $[-\pi, \pi)$. Hence, $G(\varphi_x)$ is equal to G_{m} with probability $\bar{w} = \frac{w}{2\pi}$ and G_{s} with probability $1 - \bar{w}$. Without loss of generality, the noise power is set to one, and the SINR at the typical receiver is then given by

$$\mathrm{SINR} = \frac{\mu G_{\mathrm{m}} h_{x_0} r_0^{-\alpha_{\mathrm{L}}}}{1 + \sum\limits_{x\in\Phi} \mu G(\varphi_x) h_x \ell(x) B_x}. \tag{5}$$

III. A General Framework for Fine-Grained Analysis of mm-wave D2D Networks

In this section, we will develop a general framework for the fine-grained analysis of mm-wave D2D networks. The main results include the exact analytical expression and a general beta approximation for the meta distribution of the typical D2D receiver, which will then be applied in the analysis of the local delay and the SOC for mm-wave D2D networks.

A. Meta Distribution of the SINR

The meta distribution of the SINR is a two-parameter distribution function defined as [17]

$$\bar{F}_{\mathrm{P_s}(\theta)}(x) \triangleq \mathbb{P}_o^!(\mathrm{P_s}(\theta) > x),\ \theta \in \mathbb{R}^+,\ x \in [0, 1]. \tag{6}$$

[1]Note that the LOS mm-wave links are better modeled by the Nakagami fading. However, we resort to Rayleigh fading as it enables much better tractability. In addition, simulation results in Sec. IV show that Nakagami and Rayleigh fading present the same trends in terms of SINR performance.

[2]With the standard path loss law $r^{-\alpha}$, for $\alpha \le 2$, the interference is infinite almost surely unless the network considered is finite, while for $\alpha > 2$, the interference is finite but with infinite mean due to the singularity of the path loss law at the origin [23]. Accordingly, in our system model, we assume $\alpha_{\mathrm{N}} > \max(\alpha_{\mathrm{L}}, 2)$.

which represents the complementary cumulative distribution function (CCDF) of the link success probability $P_{\rm s}(\theta)$ conditioned on the point process. Here $\mathbb{P}_o^!$ denotes the reduced Palm probability conditioning on the typical receiver at the origin o and its corresponding transmitter to be active, and the link success probability $P_{\rm s}(\theta)$ is a random variable given as

$$P_{\rm s}(\theta) \triangleq \mathbb{P}(\text{SINR} > \theta \mid \Phi), \tag{7}$$

where θ is the SINR threshold. Due to the ergodicity of the point process, the meta distribution can be interpreted as the fraction of links in each realization of the point process that have a SINR greater than θ with probability at least x. By such a definition, the standard success probability is the mean of $P_{\rm s}(\theta)$, obtained by integrating the meta distribution (6) over $x \in [0,1]$. Since a direct calculation of the meta distribution seems infeasible, we will derive the exact analytical expression through the moments $M_b(\theta) \triangleq \mathbb{E}\left[P_{\rm s}(\theta)^b\right]$ first and then approximate it with much simpler closed-form expressions.

Theorem 1. (Moments for mm-wave D2D network with ALOHA) *Given that the typical link is LOS and active, the moment M_b ($b \in \mathbb{C}$) of the conditional success probability in mm-wave D2D networks is*

$$M_b(\theta) = \exp\left(-\lambda\pi R^2(1 - p_{\rm L}A_{\rm L} - p_{\rm N}A_{\rm N}) - \frac{b\theta r_0^{\alpha_{\rm L}}}{\mu G_{\rm m}}\right), \tag{8}$$

where

$$A_i = \sum_{n=0}^{\infty}\binom{b}{n}(-p)^n \sum_{m=0}^{n}\binom{n}{m}\bar{w}^m(1-\bar{w})^{n-m}F_{m,n-m}(\alpha_i,\theta), \tag{9}$$

and

$$F_{m,n-m}(\alpha_i,\theta) = \tilde{F}_1\left(\delta_i, m, n-m, \delta_i+1, \frac{-R^{\alpha_i}}{\theta r_0^{\alpha_{\rm L}}}, \frac{-G_{\rm m}R^{\alpha_i}}{G_{\rm s}\theta r_0^{\alpha_{\rm L}}}\right). \tag{10}$$

Here $\tilde{F}_1(\cdot)$ is the hypergeometric function of two variables[3] *[24, Chap. 9.18] and $\delta_i = 2/\alpha_i$, $i \in \{\rm L, N\}$.*

Proof: See Appendix A.

The first moment of the conditional success probability is the standard success probability for the mm-wave D2D network, denoted as $p_{\rm s}(\theta)$ or $M_1(\theta)$. It is given as

$$p_s(\theta) = M_1(\theta) = \exp\left(-\lambda p\pi R^2(p_{\rm L}\xi_1^{\rm L} + p_{\rm N}\xi_1^{\rm N}) - \frac{\theta r_0^{\alpha_{\rm L}}}{\mu G_{\rm m}}\right), \tag{11}$$

where

$$\xi_1^i = \bar{w}\ {}_2F_1\left(1, \delta_i, \delta_i+1, \frac{-R^{\alpha_i}}{\theta r_0^{\alpha_{\rm L}}}\right) + (1-\bar{w}) \times {}_2F_1\left(1, \delta_i, \delta_i+1, \frac{-G_{\rm m}R^{\alpha_i}}{G_{\rm s}\theta r_0^{\alpha_{\rm L}}}\right),\ i \in \{\rm L, N\}. \tag{12}$$

When $\alpha_{\rm L} = 2$ and $\alpha_{\rm N} = 4$, we have the simpler expressions

$$\xi_1^{\rm L} = \bar{w}\frac{\theta r_0^2}{R^2}\ln\left(1+\frac{R^2}{\theta r_0^2}\right) + (1-\bar{w})\frac{G_{\rm s}\theta r_0^2}{G_{\rm m}R^2}\ln\left(1+\frac{G_{\rm m}R^2}{G_{\rm s}\theta r_0^2}\right),$$

$$\xi_1^{\rm N} = \bar{w}\frac{\sqrt{\theta}r_0}{R^2}\arctan\left(\frac{R^2}{\sqrt{\theta}r_0}\right) + (1-\bar{w})\frac{\sqrt{G_{\rm s}\theta}r_0}{\sqrt{G_{\rm m}}R^2}\arctan\left(\frac{\sqrt{G_{\rm m}}R^2}{\sqrt{\theta G_{\rm s}}r_0}\right).$$

[3]The $\tilde{F}_1$ function is also called the Appell function and is implemented in the Wolfram Language as **AppellF1**$[a, b_1, b_2, c, x, y]$.

The second moment of the conditional success probability is given as

$$M_2(\theta) = (M_1(\theta))^2 \exp\left(\lambda p^2\pi R^2(p_{\rm L}\xi_2^{\rm L} + p_{\rm N}\xi_2^{\rm N})\right), \tag{13}$$

where

$$\xi_2^i = \bar{w}^2\ {}_2F_1\left(2, \delta_i, \delta_i+1, \frac{-R^{\alpha_i}}{\theta r_0^{\alpha_{\rm L}}}\right) + 2\bar{w}(1-\bar{w})F_{1,1}(\alpha_i,\theta) + (1-\bar{w})^2\ {}_2F_1\left(2, \delta_i, \delta_i+1, \frac{-G_{\rm m}R^{\alpha_i}}{G_{\rm s}\theta r_0^{\alpha_{\rm L}}}\right),\ i \in \{\rm L, N\}. \tag{14}$$

When $\alpha_{\rm L} = 2$ and $\alpha_{\rm N} = 4$, we have

$$\xi_2^{\rm L} = \frac{\bar{w}^2\theta r_0^2}{\theta r_0^2 + R^2} + \frac{(1-\bar{w})^2 G_{\rm s}\theta r_0^2}{G_{\rm s}\theta r_0^2 + G_{\rm m}R^2} + \frac{2\bar{w}(1-\bar{w})G_{\rm s}\theta r_0^2}{(G_{\rm m}-G_{\rm s})R^2}\ln\left(\frac{G_{\rm s}\theta r_0^2 + G_{\rm m}R^2}{G_{\rm s}\theta r_0^2 + G_{\rm s}R^2}\right),$$

$$\xi_2^{\rm N} = \frac{\bar{w}^2}{2}\left(\frac{\sqrt{\theta}r_0}{R^2}\arctan\frac{R^2}{\sqrt{\theta}r_0} + \frac{\theta r_0^2}{\theta r_0^2 + R^4}\right) + \frac{(1-\bar{w})^2}{2}\left(\frac{\sqrt{G_{\rm s}\theta}r_0}{R^2}\arctan\frac{R^2}{\sqrt{\theta}r_0} + \frac{\theta r_0^2}{\theta r_0^2 + R^4}\right) + \frac{2\bar{w}(1-\bar{w})G_{\rm s}\sqrt{\theta}r_0}{(G_{\rm m}-G_{\rm s})R^2}\left(\arctan\frac{\sqrt{G_{\rm m}}R^2}{\sqrt{G_{\rm s}\theta}r_0} - \arctan\frac{R^2}{\sqrt{\theta}r_0}\right).$$

The variance of the conditional success probability can be obtained as $\text{var}\, P_{\rm s}(\theta) = M_2(\theta) - M_1^2(\theta)$. As in [17], we also find in mm-wave D2D networks that the same λp leads to the same standard success probability but the variance depends on both λ and p, not just the product, which highlights the importance of the fine-grained analysis based on the meta distribution. Moreover, in mm-wave D2D networks, as in bipolar networks with standard path loss and single-antenna nodes, we also have the following concentration property.

Corollary 1. (Concentration as $p \to 0$) *Keeping the transmitter density $t \triangleq \lambda p$ fixed and letting $p \to 0$, we have*

$$\lim_{p\to 0, \lambda p = t} P_{\rm s}(\theta) = M_1(\theta) = p_{\rm s}(\theta) \tag{15}$$

in mean square (and probability and distribution).

Proof: From the expression of ξ_2^i in (17), when $p \to 0$, we have $\xi_2^i = 2\xi_1^i$ and thus $M_2(\theta) = M_1^2(\theta)$. In this case, the limiting variance is zero, i.e.,

$$\lim_{p\to 0, \lambda p = t} \text{var}\, P_{\rm s}(\theta) = 0. \tag{16}$$

■

The concentration property means that in the limit of a very dense network with very small p, all links in the network have exactly the same success probability (or reliability).

For mm-wave networks, it is very important and interesting to explore how the performance changes with the antenna array size N and what happens when extremely massive antenna arrays are used, i.e., as $N \to \infty$. Both questions are answered in the following corollary.

Corollary 2. (Monotonicity with N) *For $b \in \mathbb{R}^+$, M_b is monotonically increasing with N. When $N \to \infty$, M_b is given by*

$$\lim_{N\to\infty} M_b(\theta) = \exp\left(-\lambda\pi R^2(p_{\rm L}A_{\rm L} + p_{\rm N}A_{\rm N})\right), \quad b \in \mathbb{C}, \tag{17}$$

where

$$A_i = \sum_{n=1}^{\infty} \binom{b}{n} (-1)^{n+1} p^n \, {}_2F_1\left(n, \delta_i, \delta_i+1, \frac{9\pi^2 R^{\alpha_i}}{4\theta r_0^{\alpha_{\rm L}}}\right). \quad (18)$$

Here ${}_2F_1(\cdot)$ is the Gaussian hypergeometric function [24, Chap. 9.11], and $\delta_i = 2/\alpha_i$, $i \in \{\mathrm{L}, \mathrm{N}\}$.

Proof: See Appendix B.

So when $N \to \infty$, we obtain an upper limit of the standard success probability $M_1(\theta)$ as

$$\lim_{N\to\infty} M_1(\theta) = \exp\left(-\lambda p \pi R^2 \sum_{i\in\{\mathrm{L},\mathrm{N}\}} p_i \, {}_2F_1\left(1, \delta_i, \delta_i+1, \frac{-9\pi^2 R^{\alpha_i}}{4\theta r_0^{\alpha_{\rm L}}}\right)\right). \quad (19)$$

This corollary implies that the standard success probability improves with increasing N and converges to its maximum as $N \to \infty$. Furthermore, the limit (17) also provides the following insights: (1) As $N \to \infty$, the effect of the noise is totally suppressed since $G_{\rm m} \to \infty$; (2) The side lobe interference gradually becomes the main performance-limiting factor as $N \to \infty$. In this regime, the node density plays a critical role in determining the interference power in the network. For instance, a sparse network makes the interference in a massive MIMO network arbitrarily small while a dense one is interference-limited.

The exact meta distribution can be obtained by the Gil-Pelaez theorem [25] with the imaginary moments M_{jt} of $P_{\rm s}(\theta)$, $t \in \mathbb{R}$, $j \triangleq \sqrt{-1}$.

Corollary 3. (Exact expression) *The meta distribution for the mm-wave D2D networks is given by*

$$\bar{F}_{P_s(\theta)}(x) = \frac{1}{2} - \frac{1}{\pi}\int_0^{\infty} \frac{e^{-\lambda\pi R^2(1-\Re(\zeta))}}{t} \times \sin\left(t\log x + t\frac{\theta r_0^{\alpha_{\rm L}}}{\mu G_{\rm m}} - \lambda\pi R^2 \Im(\zeta)\right) \mathrm{d}t, \quad (20)$$

where $\zeta = p_{\rm L}A_{\rm L} + p_{\rm N}A_{\rm N}$ is given in (9) with $b = jt$ and $\Re(z)$ and $\Im(z)$ denote the real and imaginary parts of $z \in \mathbb{C}$, respectively.

Proof: According to the Gil-Pelaez theorem, the ccdf of $P_s(\theta)$ is given by

$$\bar{F}_{P_s(\theta)}(x) = \frac{1}{2} + \frac{1}{\pi}\int_0^{\infty} \frac{\Im\left(e^{-jt\log x} M_{jt}\right)}{t} \mathrm{d}t, \quad (21)$$

where M_{jt}, $t \in \mathbb{R}$ is given in (8), and $\Im(z)$ is the imaginary part of $z \in \mathbb{C}$. Letting $\zeta = p_{\rm L}A_{\rm L} + p_{\rm N}A_{\rm N}$, we have

$$\begin{aligned}
&\bar{F}_{P_s(\theta)}(x) \\
&= \frac{1}{2} + \frac{1}{\pi}\int_0^{\infty} \Im\left(e^{-jt\log x} e^{-\lambda\pi R^2(1-\zeta) - jt\theta r_0^{\alpha_{\rm L}}/(\mu G_{\rm m})}\right) \frac{1}{t}\mathrm{d}t \\
&= \frac{1}{2} + \frac{1}{\pi}\int_0^{\infty} \frac{e^{-\lambda\pi R^2(1-\Re(\zeta))}}{t} \Im\left(e^{-jt\log x} e^{j\lambda\pi R^2\Im(\zeta) - jt\frac{\theta r_0^{\alpha_{\rm L}}}{\mu G_{\rm m}}}\right) \mathrm{d}t \\
&= \frac{1}{2} - \frac{1}{\pi}\int_0^{\infty} e^{-\lambda\pi R^2(1-\Re(\zeta))} \sin\left(t\log x + \frac{t\theta r_0^{\alpha_{\rm L}}}{\mu G_{\rm m}} - \lambda\pi R^2\Im(\zeta)\right) \frac{1}{t}\mathrm{d}t.
\end{aligned}$$

■

B. Approximations of the Meta Distribution

Though the expression in Cor. 3 is exact and can be calculated via numerical integration techniques, it is difficult to gain insights directly and apply it to obtain other analytical results. To approximate the meta distribution, we first use the same approach adopted in [17] by matching the mean and variance of the beta distribution with $M_1(\theta)$ and $M_2(\theta)$ given in Theorem 1 to verify whether this approximation is also acceptable for mm-wave D2D networks, where the interference characteristics are different from those in microwave networks. The probability density function (PDF) of a beta distributed random variable X with parameters κ and β is

$$f_X(x) = \frac{x^{\kappa-1}(1-x)^{\beta-1}}{B(\kappa,\beta)}, \quad (22)$$

where $B(\cdot,\cdot)$ is the beta function. The first and second moment of X are given as

$$\mathbb{E}X = \frac{\kappa}{\kappa+\beta}, \quad \mathbb{E}(X^2) = \frac{\kappa+1}{\kappa+\beta+1}\mathbb{E}X. \quad (23)$$

Letting $\mathbb{E}X = M_1(\theta)$ and $\mathbb{E}(X^2) = M_2(\theta)$, we have

$$\kappa = \frac{M_1 M_2 - M_1^2}{M_1^2 - M_2}, \quad \beta = \frac{(1-M_1)(M_2-M_1)}{M_1^2 - M_2}. \quad (24)$$

Hence, the approximate meta distribution of the typical mm-wave D2D receiver follows as

$$\bar{F}_{P_s(\theta)}(x) \approx 1 - I_x(\kappa,\beta), \quad (25)$$

where $I_x(\kappa,\beta)$ is the regularized incomplete beta function.

To answer the question when the above approximation provides a good match with the exact result in mm-wave networks and when not, we compare them with different numbers of antenna elements N and node densities in Fig. 1(a). It is observed that the standard beta distribution provides an excellent match for the case with severe interference while as the number of antennas increases with narrower beams or the density of the nodes decreases, the approximations start to deviate from the exact results. The smaller the interference, the larger the deviations. However, due to the unique features of mm-wave such as high propagation loss, highly directional transmission, and sensitivity to blockage, the interference behavior is different from the microwave communications. The randomness of the interference stems from the spatial relative locations between the interferer and the receiver or the interfering beam directions. Due to the randomness of the distribution of the D2D users, both strong and weak interference scenarios will occur. Thus, for the sake of approximating the meta distribution more accurately even for the light interference scenarios in mm-wave bands, we propose another approximation with a generalized beta distribution whose PDF with parameters (κ,β,ρ) is given as

$$f_X(x) = \frac{x^{\kappa-1}(1-x/\rho)^{\beta-1}}{\rho^{\kappa}B(\kappa,\beta)}\mathbf{1}_{x\le\rho}, \quad (26)$$

where $\rho \in (0,1]$. Clearly, for $\rho = 1$, this reverts to the standard beta approximation. The parameters can also be obtained through the moment matching method, given as

$$\mathbb{E}X = \frac{\rho\kappa}{\kappa+\beta}, \quad \mathbb{E}(X^n) = \rho\frac{\kappa+n-1}{\kappa+\beta+n-1}\mathbb{E}(X^{n-1}), \quad (27)$$

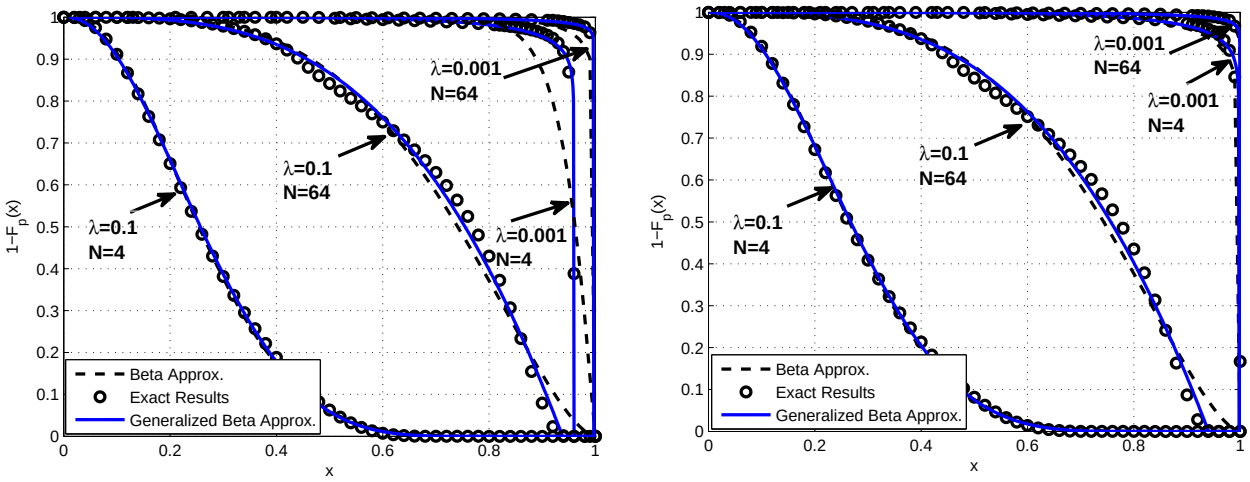

(a) SINR analysis

(b) SIR analysis

Fig. 1. Standard beta approximation versus generalized beta approximation with $p_{\rm L} = 0.2, r_0 = 3, \mu = 20, p = 0.5, \alpha_{\rm L} = 2.5, \alpha_{\rm N} = 4$.

and the solutions to the three equations, i.e., $n = 1, 2, 3$ can be easily obtained via the **fsolve** function in Matlab 2014 (and later versions). Thus, the generalized beta approximation of the meta distribution is obtained by

$$\bar{F}_{P_s(\theta)}(x) \approx (1 - I_x(\kappa/\rho, \beta))\mathbf{1}_{x \le \rho}. \tag{28}$$

From the numerical results in Fig. 1, we find that the generalized beta approximation provides an excellent match for the distribution of the link success probability with a wider range of application. For example, for $N = 64$, when a highly directional antenna array is adopted, the generalized beta approximation provides a more accurate match than the standard beta distribution, especially at high reliabilities. Moreover, from $\lambda = 0.1$ to $\lambda = 0.001$, when the node density decreases, the deviation of the standard beta distribution becomes quite significant while the generalized beta approximation still provides an excellent match.

Furthermore, to investigate how the noise affects the meta distribution and its approximation, we compare the meta distributions of the SINR and the SIR, where the latter is the noiseless case, shown in Fig. 1(b). It is seen that the meta distribution for weak interference is truncated at $x < 1$ in case (a) but not in case (b), see the two curves with $\lambda = 0.001$ in each figure. This phenomenon indicates that when the node density decreases, the network tends to be noise-limited, and the effect of the noise on the meta distribution cannot be ignored. This is also the reason why $\rho < 1$ in (26) leads to a better fit for the SINR analysis. Besides, as explained for Cor. 2, when N becomes larger, the node density becomes the dominant factor of the interference. Thus, when $N = 64$, due to the higher node density $\lambda = 0.1$, even though the noise effect is not considered, the meta distribution is also truncated before 1 but now because of the interference. This indicates that for the mm-wave network with large antenna arrays and dense deployment, the standard beta distribution does not provide an accurate approximation of the meta distribution especially at high reliabilities (near 1), whereas the generalized one does.

In summary, by using higher moments of the conditional SINR distribution, the generalized beta approximation provides an excellent match for the distribution of the link success probability with a wider range of application scenarios (both interference-limited and noise-limited cases) and reverts to the standard one for $\rho = 1$. Such a quick and efficient approximation significantly facilitates the performance evaluation, which will play an important role for network planning and management.

C. Meta Distribution of the Data Rate

In addition to the transmission reliability (or the success probability), the data rate, characterized by the rate distribution, is another fundamental performance metric of transmission effectiveness. Denote T as the (random) data rate of the typical link, with unit of bps. According to the Shannon capacity formula $T = W \log_2(1 + \mathrm{SINR})$, we have the rate distribution $\mathbb{P}(T > \tau) = M_1(2^{\tau/W} - 1)$. Similar to the meta distribution of the SINR, conditioned on the point process, we can also derive the meta distribution of the data rate $\bar{F}_T(\tau, x)$ to present the fraction of active users in each realization of the point process that have a rate T greater than τ with probability at least x.

Theorem 2. (Meta distribution of data rate for mm-wave D2D receivers) *Given that the typical link is LOS and active, the meta distribution of the data rate in mm-wave D2D networks can be obtained through the moment S_b $(b \in \mathbb{C})$ of the conditional data rate, where $S_b(\tau) = M_b(2^{\tau/W} - 1)$.*

Proof: Since $T = W \log_2(1 + \mathrm{SINR})$, we have

$$\begin{aligned} \mathbb{P}(T > \tau \mid \Phi) &= \mathbb{P}(W \log_2(1 + \mathrm{SINR}) > \tau \mid \Phi) \\ &= \mathbb{P}(\mathrm{SINR} > 2^{\tau/W} - 1 \mid \Phi). \end{aligned} \tag{29}$$

Therefore,

$$S_b(\tau) = \mathbb{E}_\Phi \left[\left(\mathbb{P}(\mathrm{SINR} > 2^{\tau/W} - 1 \mid \Phi) \right)^b \right]$$

$$= \quad M_b(2^{\tau/W}-1). \tag{30}$$

■

The first moment of the conditional data rate is the rate distribution for the mm-wave D2D network, given as

$$S_1(\tau)=\exp\left(-\lambda p\pi R^2(p_{\rm L}\xi_1^{\rm L}+p_{\rm N}\xi_1^{\rm N})-\frac{\widetilde{\tau}r_0^{\alpha_{\rm L}}}{\mu G_{\rm m}}\right), \tag{31}$$

where $\widetilde{\tau}=2^{\tau/W}-1$, and

$$\begin{aligned}\xi_1^i \;=\; & \bar{w}\,{}_2F_1\left(1,\delta_i,\delta_i+1,\frac{-R^{\alpha_i}}{\widetilde{\tau}r_0^{\alpha_{\rm L}}}\right)\\ & +(1-\bar{w})\,{}_2F_1\left(1,\delta_i,\delta_i+1,\frac{-G_{\rm m}R^{\alpha_i}}{G_{\rm s}\widetilde{\tau}r_0^{\alpha_{\rm L}}}\right), i\in\{\rm L,N\}.\end{aligned}$$

The exact meta distribution $\bar{F}_T(\tau,x)$ of the data rate can also be calculated via the Gil-Pelaez theorem. Due to the similarity of the meta distribution between the SINR and achievable rate, the beta approximation also works well in some regimes, and the generalized beta approximation is accurate in all cases we considered.

D. The Mean and Variance of the Local Delay

The local delay is another important network performance metric that directly affects the perceived experience of users. It is defined as the number of transmission attempts needed until the first success [26]. In each transmission attempt, the transmitter is allowed to transmit with probability p, and the transmission will be successful with probability $P_{\rm s}(\theta)$ conditioned upon Φ. Therefore, the transmission attempts are independent (Bernoulli) trials with success probability $pP_{\rm s}(\theta)$ and the conditional local delay, denoted as $D_\Phi=(D\mid\Phi)$, is a random variable with geometric distribution given by

$$\mathbb{P}(D_\Phi=k)=(1-pP_{\rm s}(\theta))^{k-1}pP_{\rm s}(\theta). \tag{32}$$

Hence the mean conditional local delay is given by $\mathbb{E}D_\Phi=\frac{1}{pP_{\rm s}(\theta)}$. As a result, the mean local delay $\bar{D}$ is obtained as $\bar{D}=\mathbb{E}\big((pP_{\rm s}(\theta))^{-1}\big)=\frac{1}{p}M_{-1}$, which characterizes the mean number of transmission attempts needed until a packet is successfully transmitted. The specific expression of the mean local delay is given as follows.

Theorem 3. *Letting $v_i=\frac{R^{\alpha_i}}{\theta r_0^{\alpha_{\rm L}}}$ and $\tilde{v}_i=\frac{v_iG_{\rm m}}{G_{\rm s}}$, the mean local delay $\bar{D}$ of mm-wave D2D networks is*

$$\begin{aligned}\bar{D}=\frac{1}{p}\exp\Bigg(&\frac{\theta r_0^{\alpha_{\rm L}}}{G_{\rm m}\mu}+\sum_{i\in\{\rm L,N\}}\lambda p\pi R^2p_i\Bigg(\tilde{F}(\delta_i,1,1,\delta_i+1,z_1,z_2)\\ &+\frac{\delta_i(\bar{w}\tilde{v}_i+(1-\bar{w})v_i)}{\delta_i+1}\tilde{F}(\delta_i+1,1,1,\delta_i+2,z_1,z_2)\Bigg)\Bigg),\end{aligned} \tag{33}$$

where $\frac{1}{z_1}$ and $\frac{1}{z_2}$ are the two different real roots of $f(y)=v_i\tilde{v}_iy^2+(v_i+\tilde{v}_i-p\bar{w}\tilde{v}_i-p(1-\bar{w})v_i)y+1-p$.

Proof: See Appendix C.

In order to better understand the distribution of the local delay, we also derive its variance to characterize the fluctuation of the delay (or jitter).

Theorem 4. *Letting $v_i=\frac{R^{\alpha_i}}{\theta r_0^{\alpha_{\rm L}}}$ and $\tilde{v}_i=\frac{v_iG_{\rm m}}{G_{\rm s}}$, the variance of the local delay $V(D)$ in mm-wave D2D networks is*

$$\begin{aligned}V(D)=&\frac{2}{p^2}\bar{D}^2\exp\Bigg(\lambda p^2\pi R^2\sum_{i\in\{\rm L,N\}}p_i\Bigg(\tilde{F}(\delta_i,2,2,\delta_i+1,z_1,z_2)\\ &+\frac{2\delta_i(\bar{w}\tilde{v}_i+(1-\bar{w})v_i)}{\delta_i+1}\tilde{F}(\delta_i+1,2,2,\delta_i+2,z_1,z_2)\\ &+\frac{\delta_i(\bar{w}\tilde{v}_i+(1-\bar{w})v_i)^2}{\delta_i+2}\tilde{F}(\delta_i+2,2,2,\delta_i+3,z_1,z_2)\Bigg)\Bigg)\\ &-\bar{D}-\bar{D}^2,\end{aligned} \tag{34}$$

where $\frac{1}{z_1}$ and $\frac{1}{z_2}$ are the two different real roots of $f(y)=v_i\tilde{v}_iy^2+(v_i+\tilde{v}_i-p\bar{w}\tilde{v}_i-p(1-\bar{w})v_i)y+1-p=0$.

Proof: See Appendix D.

E. Spatial Outage Capacity

The *spatial outage capacity* (SOC), introduced in [20], is a new notion of capacity that can be calculated using the meta distribution. The SOC is defined as the maximum density of concurrently active links with a success probability greater than a certain threshold. According to the definition, the SOC of mm-wave D2D networks is given by

$$S(\theta,x)\triangleq\sup_{\lambda>0,p\in(0,1]}\lambda p\bar{F}_{P_{\rm s}(\theta)}(x),\ \theta>0,\ x\in(0,1). \tag{35}$$

The SOC measures the maximum density of links that satisfy a certain reliability requirement in a mm-wave D2D network, where the reliability requirement is applied at each individual link given the SINR threshold θ. We denote the density of concurrently active links that have a success probability greater than x as

$$s(\theta,x)\triangleq\lambda p\bar{F}_{P_{\rm s}(\theta)}(x). \tag{36}$$

With the accurate approximation of the generalized beta distribution above, $s(\theta,x)$ is approximated as

$$s(\theta,x)\approx\lambda p(1-I_x(\kappa/\rho,\beta))\mathbf{1}_{x\le\rho}. \tag{37}$$

It should be noted that both the meta distribution and the SOC are important performance metrics: the former characterizes a fine-grained link-level performance of all links (i.e., the entire distribution of the random variable instead of just the mean); while the latter characterizes a fine-grained network-level performance (i.e., the maximum density for a network with a certain QoS constraint applied at each individual link instead of the standard area spectral efficiency (ASE) which is just the mean achievable rate per unit area given that the typical link satisfies the QoS constraint). Thus, from these two performance metrics, we capture the performance of individual links and obtain much sharper results than merely the SINR and ASE at the typical user.

IV. Numerical Results

In this section, we will present numerical results of various performance metrics involved in the framework in Section III for mm-wave D2D networks. The main symbols and parameters are summarized in Table II with default values in the simulations.

TABLE II. Symbols and descriptions

Symbol	Description	Default value
Φ, λ	mm-wave device PPP and density	$\mathrm{N/A}, 0.1/\mathrm{m}^2$
μ	The transmit power	20 dB
W	mm-wave bandwidth	2GHz
r_0	The link distance between the D2D users	3m
p	The transmit probability in each time slot	0.5
$p_{\mathrm{L}}/p_{\mathrm{N}}$	The probability of a link being LOS/NLOS	0.2/0.8
$\alpha_{\mathrm{L}}/\alpha_{\mathrm{N}}$	The path loss exponent of the LOS/NLOS link	2.5/4
R	The radius of the generalized LOS ball	200m
θ	The SINR threshold	0 dB
$G_{\mathrm{m}}/G_{\mathrm{s}}$	The main lobe/side lobe of the antenna pattern	N/A
w	The beam-width of the antenna pattern	N/A
$\bar{F}_{P_{\mathrm{s}}(\theta)}(x)/\bar{F}_T(x,\tau)$	The meta distribution of the SINR/data rate	N/A
M_b/M_b^{τ}	The b-th moments of the conditional SINR/data rate distribution	N/A

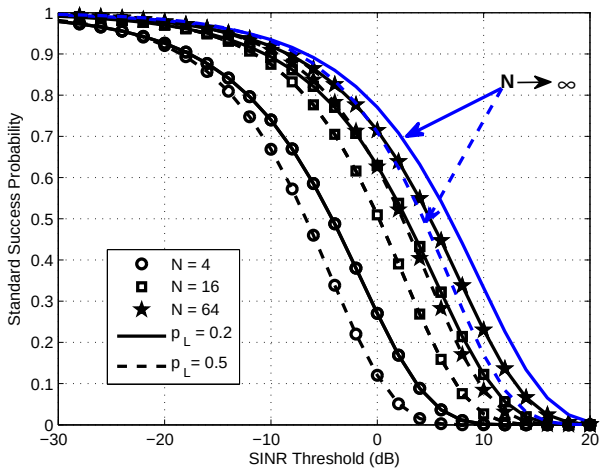

Fig. 2. The standard success probability M_1.

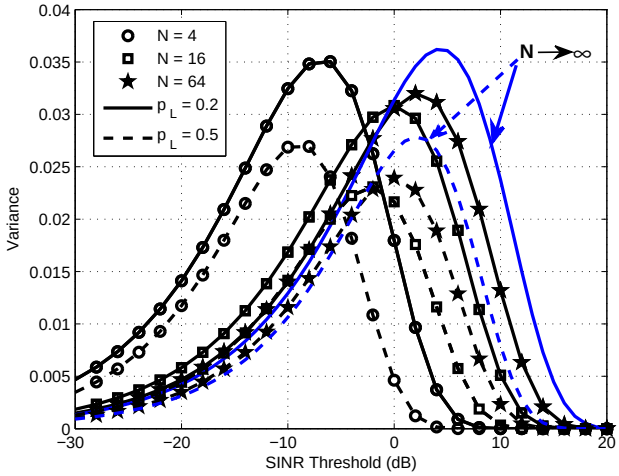

Fig. 3. The variance $M_2 - M_1^2$ of the conditional success probability.

A. The Impact of mm-Wave Features

Directional transmission and sensitivity to blockage are two key features of mm-wave communication. In this subsection, we focus on the impacts of the LOS probability p_{L} and antenna array size N on the mean and variance of the conditional success probability $P_{\mathrm{s}}(\theta)$. Moreover, we also investigate the interference behaviors under various mm-wave D2D scenarios.

As shown in Fig. 2, increasing the number of antennas improves the standard success probability due to the fact that a larger antenna array can form a narrower beam, thus causing less interference. As the number of antennas tends to infinity, the standard success probability converges to an upper limit (see Cor. 2), since the side-lobe leakage restricts the performance improvement. However, for the LOS probability, a higher p_{L} means the number of LOS links is larger, leading to more severe interference. Thus, the standard success probability deteriorates with the increase of p_{L}.

Fig. 3 presents the variance of the conditional success probability as a function of θ for different LOS probabilities and antenna array sizes. Since the variance necessarily tends to zero for both $\theta \to 0$ and $\theta \to \infty$, it assumes a maximum at some finite value of θ. It can be seen that given a p_{L}, the θ with the maximum variance increases with N and converges to an upper limit, similar to M_1. Moreover, there is no monotonicity of the variance with respect to N. For example, for $\theta = -10$ dB, the variance decreases with increasing N, while the opposite happens for $\theta = 10$ dB. We also find that a larger p_{L} leads to smaller variance. The reason is that in LOS environment with smaller path loss exponent, the randomness of the relative distances of the interferers and the receiver has a smaller effect on the variance of the interference than in the NLOS case.

Fig. 4 shows the relationship between the standard success probability and node density for $\theta = 0$ dB. In order to find whether and when mm-wave D2D networks are noise-limited, we also plot a SNR standard success probability where interference is neglected. As seen from the plots, the mm-wave network tends to be interference-limited as the density increases and for the given system parameters, there is a critical point $\lambda_{\mathrm{c}} \approx 10^{-4}$. The critical density λ_c is the density where the interference starts to be the dominant term in the interference-plus-noise sum, i.e., when $\mathbb{P}(I > 1)$ is high (recall that the noise power is set to 1). Therefore, when $\lambda > \lambda_{\mathrm{c}}$, the noise-limited assumption is no longer validated.

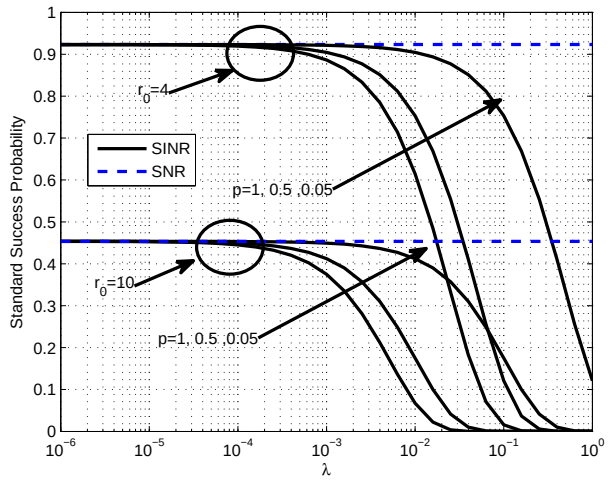

Fig. 4. Standard success probability versus density for $N = 4$.

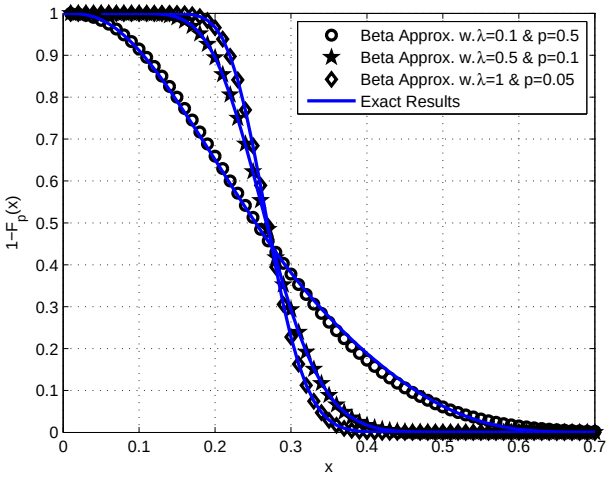

Fig. 5. Meta distribution for different λ and p with $N = 4$, $p_{\mathrm{L}} = 0.2$.

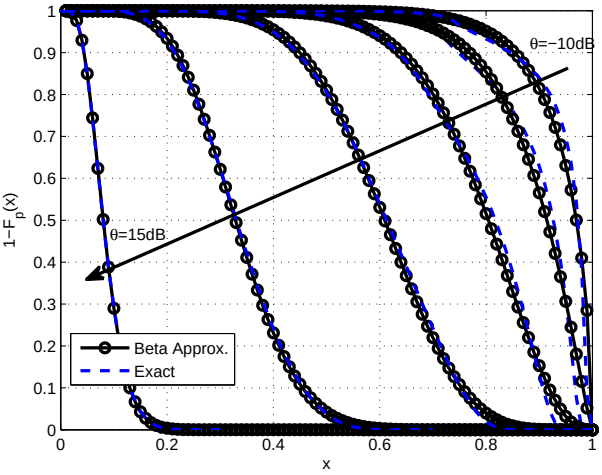

Fig. 6. Meta distribution for $\theta = -10, -5, 0, 5, 10, 15$ dB.

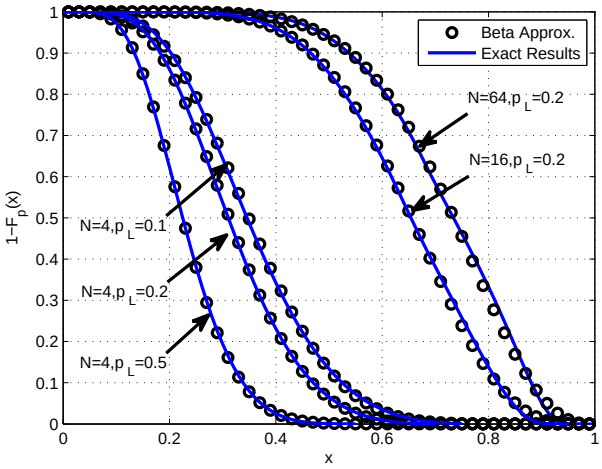

Fig. 7. Meta distribution for different p_{L} and N.

Moreover, the higher the density, the larger the deviations between the SINR and SNR performance. It is well known that D2D communication mostly applies in crowded environments such that users in close proximity can establish reliable direct communications. Therefore, it can be concluded that the mm-wave D2D network is interference-limited in most cases. Besides, the selection of the link distance between the D2D users is also important since the interferers can be arbitrarily close to the receivers; if the link distance is too large (e.g., the case $r_0 = 10$), the standard success probability will be seriously deteriorated.

B. Meta Distribution in mm-Wave Band

Fig. 5 shows comparisons of the exact results and beta approximations for $\lambda p = 0.05$ with different λ and p, respectively. As seen from the plots, for the given system parameters, the approximations match the exact results extremely well, which verifies the accuracy and the effectiveness of the approximation. Moreover, the three curves have the same value of λp and hence the same standard success probability, but the corresponding meta distributions are rather different. This shows that the standard success probability provides only limited information on the network performance.

Fig. 6 shows the meta distributions for different SINR thresholds, which enables a precise statement about what fraction of links achieve an SINR threshold with a target reliability. For example, for $\theta = -5$ dB, about 90% of the links have a success probability of at least 80%; while for $\theta = 5$ dB, less than 10% of the links achieve the same reliability.

Fig. 7 shows the impacts of LOS probability and antenna array size on the meta distribution. As seen from the plots, adopting a large antenna array boosts the performance. For example, the fractions of links with a success probability of at least 60% for $N = 16$ and $N = 64$ are about 0.7 and 0.8, respectively, which are significantly higher than for $N = 4$ where almost no links meet the requirement. In addition, similar to the standard success probability, the increase of p_{L} leads to more interferers with LOS links, thus resulting in poor performance.

Fig. 8 and Fig. 9 illustrate the rate distribution and the

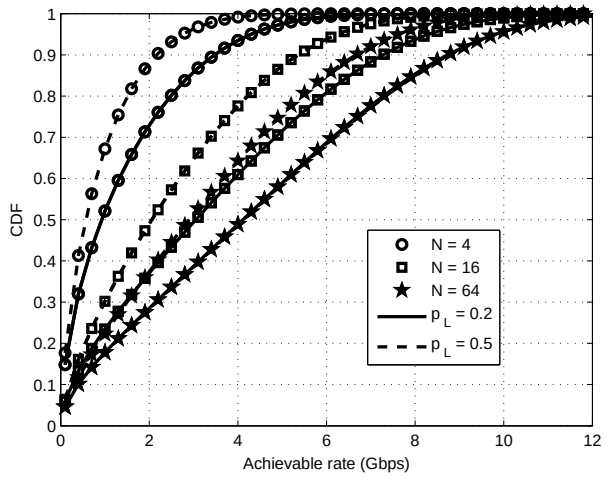

Fig. 8. The rate distribution for different N and p_{L}.

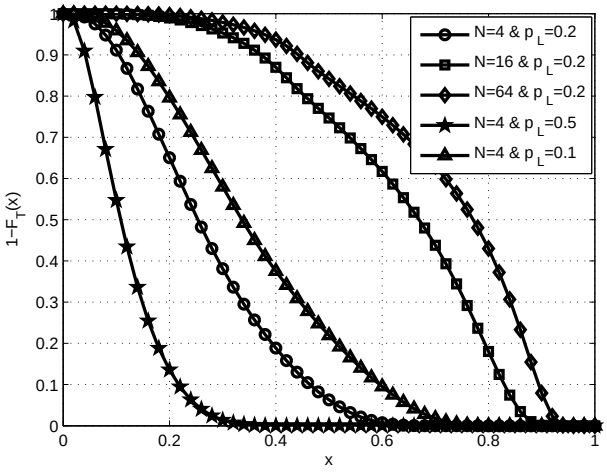

Fig. 9. Meta distribution of the achievable rate for different N and p_{L} with rate threshold $\tau = 2$ Gbps.

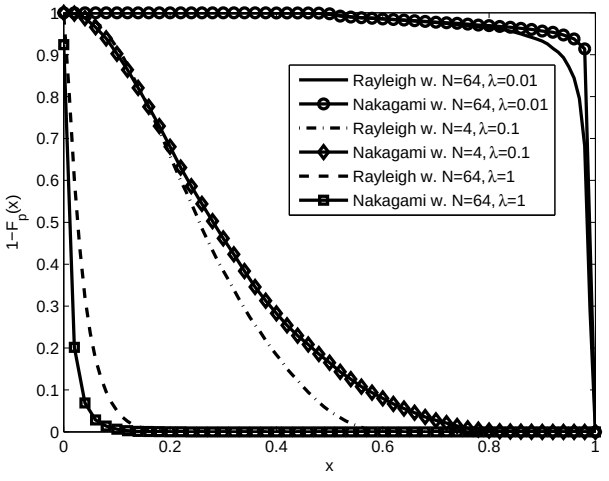

Fig. 10. Comparisons of meta distribution between Rayleigh and Nakagami-4 fading.

meta distribution of the conditional achievable rate with rate threshold $\tau = 2$ Gbps, respectively. Due to the rich bandwidth resource, for the given system parameters, mm-wave D2D communication can provide multi-gigabit-per-second rates even at moderate SINRs. This observation demonstrates the unique advantages of mm-wave communications especially for mobile broadband services. As a result, the load of the base stations and the backhaul networks could be significantly reduced. From both figures, increasing the size of the antenna array has a positive effect on the achievable rate and its meta distribution, i.e., increasing both the mean achievable rate and the fraction of concurrent links achieving a required rate. The LOS probability can also affect the path loss law of the interfering links, and thus a smaller probability leads to reduced interference. These observations help network operators find the most efficient operating regime for D2D communication in the mm-wave band.

To assess the impact of the fading model, we give a comparison of two cases: one adopts the Nakagami-m fading for LOS propagation with $m = 4$; and the other adopts the Rayleigh fading, shown in Fig. 10. It is shown that the Nakagami and Rayleigh fading present the same trends in terms of the meta distribution under different cases of densities and numbers of antennas, which implies the significance of the theoretical results based on the Rayleigh fading.

C. Mean and Variance of the Local Delay

Fig. 11 and Fig. 12 give the mean and variance of the local delay for different N and p_{L}, respectively. It can be observed that both statistics of the local delay appear to present similar trends with the transmit probability p. A small p means less opportunity to be scheduled and thus lengthens the transmission period, while a large p results in severe interference and thus reduces the successful transmission probability. Thus, both of the two cases increase the delay and jitter. Also, the optimal p that minimizes the mean local delay does not correspond to the smallest delay jitter, which highlights the importance of a fine-grained analysis for the delay performance, especially for the real-time applications which are sensitive to the delay jitter.

Moreover, the unique features of mm-wave communication, e.g., the antenna array size and the LOS probability, also have significant effects on the delay performance. As seen from the figure, a larger antenna array and a smaller LOS probability reduce the delay while maintaining the corresponding delay stability in a large range of the transmit probability, which verifies the advantages of mm-wave communications in terms of the delay performance.

D. SOC analysis

Fig. 13 explores the behavior of $s(\theta, x)$ for fixed $\theta = -10$ dB and $x = 0.9$ as a function of p and λ for different N and p_{L} and indicates the SOC point which is the combination of (λ, p) achieving the supremum of $s(\theta, x)$. It is observed that for an arbitrary combination of N and p_{L}, the SOC is always achieved at $p = 1$ under the given system parameters. Besides,

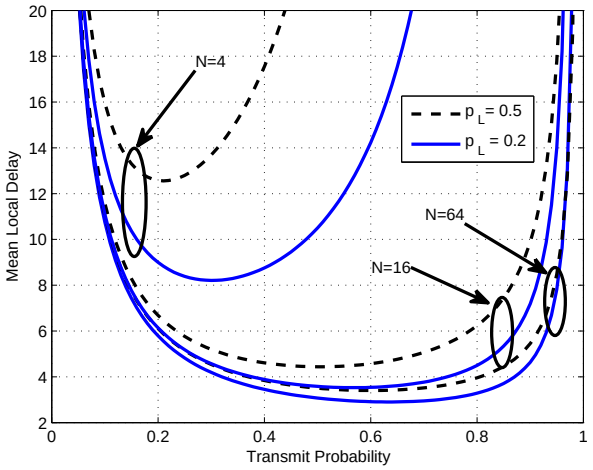

Fig. 11. The mean local delay with different N and p_{L}.

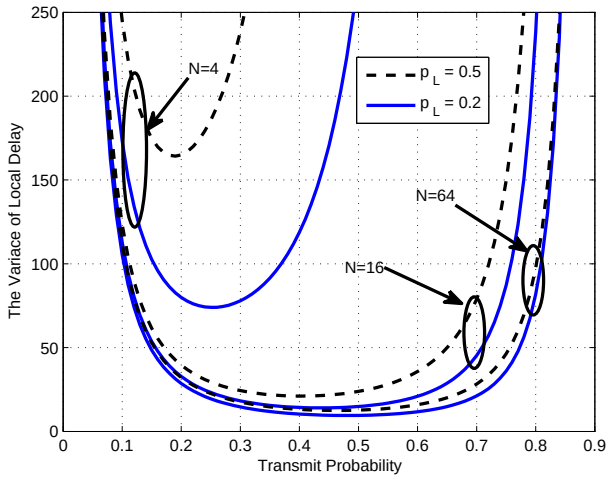

Fig. 12. The variance of the local delay with different N and p_{L}.

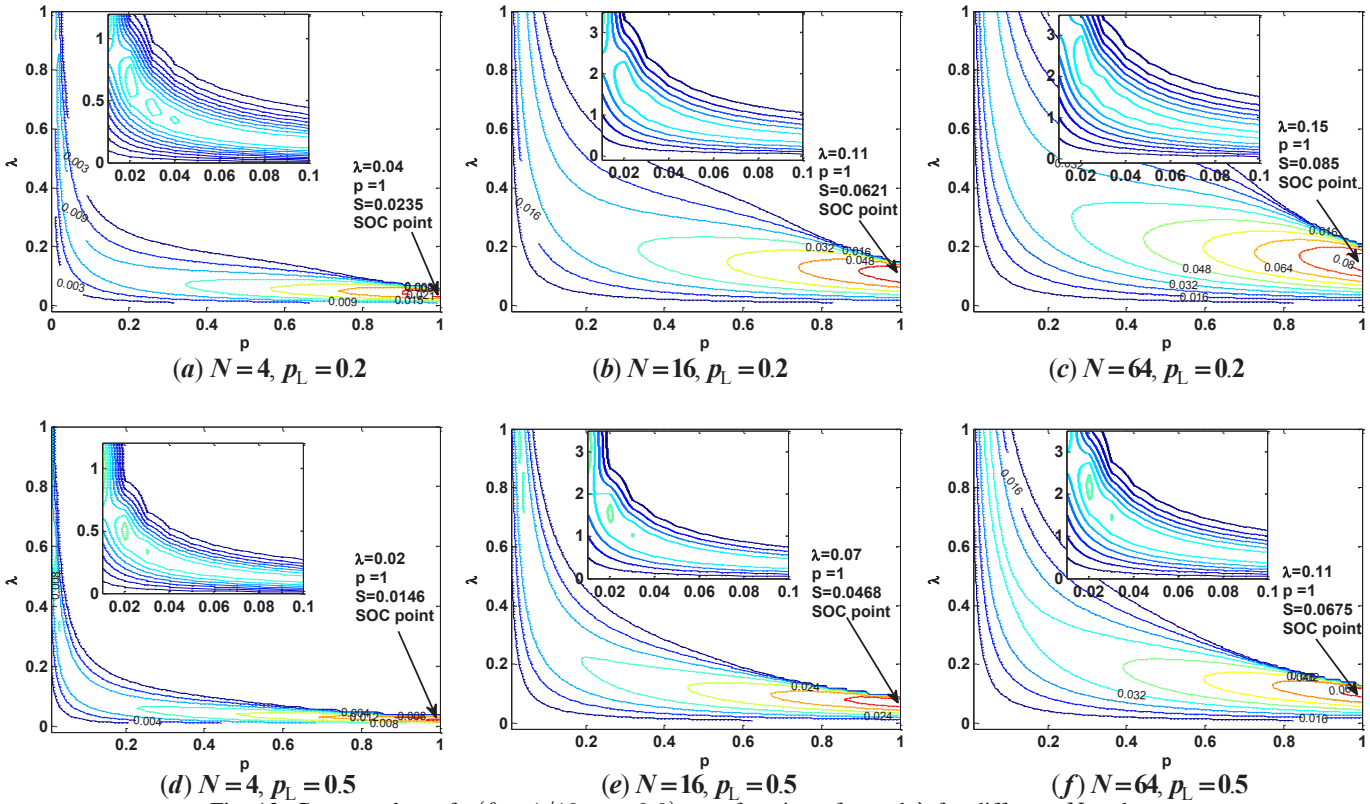

(*a*) $N=4$, $p_{\mathrm{L}}=0.2$ (*b*) $N=16$, $p_{\mathrm{L}}=0.2$ (*c*) $N=64$, $p_{\mathrm{L}}=0.2$

(*d*) $N=4$, $p_{\mathrm{L}}=0.5$ (*e*) $N=16$, $p_{\mathrm{L}}=0.5$ (*f*) $N=64$, $p_{\mathrm{L}}=0.5$

Fig. 13. Contour plots of $s(\theta=1/10, x=0.9)$ as a function of p and λ for different N and p_{L}.

given λ (or p), $s(\theta,x)$ tends to increase first to reach a critical point and then decreases as p (or λ) increases. This is because the increase of p (or λ) leads to two opposite effects on $s(\theta,x)$, namely an increase in the concurrently transmitting links λp and a decrease in the fraction $\bar{F}_{P_{\mathrm{s}}(\theta)}(x)$ of reliable links due to the increase of interference. Therefore, there exists a maximum as p (or λ) increases. It is also observed that larger N and smaller p_{L} lead to larger SOC, which can be interpreted as follows: 1) a larger N generates narrower transmitting beams concentrating more power to the dedicated receiver and thus causing less interference to other concurrent links; 2) a smaller p_{L} makes more interfering links to be NLOS, and thus the interference suffered by the receiver is also reduced. Both operations increases the fraction of successful transmission links, and thereby making the networks be able to support more concurrent links, i.e., a larger SOC can be obtained. As a baseline, the SOC serves a critical role that informs the network operator whether the mm-wave D2D network satisfies the capacity requirement.

V. Conclusions

In this paper, we propose a general framework for a fine-grained analysis of mm-wave D2D networks based on the meta distribution. We first derive the moments on the conditional success probability $P_{\rm s}$ for D2D receivers and then provide an exact expression as well as a simple yet accurate approximation for the meta distribution of the SINR. These results are then extended to the meta distribution of the achievable rate and applied to the mean and variance of the local delay as well as the SOC. Hence, the complete distribution of both the conditional link success probability and the conditional link data rate in mm-wave D2D networks can be characterized, which provides much sharper results than merely the means (i.e., the standard success probability and the mean achievable rate). Also, the SOC gives a network-level performance metric based on the meta distribution with a certain reliability constraint (or QoS requirement).

Using this framework, we fully explore the impacts of the unique features of the mm-wave band on the performance of D2D networks through both theoretical and numerical studies and obtain the following useful insights: (1) the concentration result, obtained in bipolar networks with standard path loss and single antenna, still holds in mm-wave D2D networks, i.e., the variance of $P_{\rm s}$ goes to 0 as the transmit probability $p \to 0$ while keeping the (mean) success probability constant; (2) the standard success probability increases monotonically with the antenna array size N and converges to a maximum as $N \to \infty$, where the noise is totally suppressed and the side lobe interference as well as the node density become the dominant factors in determining the interference; (3) the sensitivity to blockage is another important feature of the mm-wave band that affects the interference characteristics directly and hence the performance metrics such as the success probability, the local delay and the SOC.

In summary, the mm-wave D2D technique is expected to bring huge benefits for future wireless networks. However, the salient properties of mm-wave should be carefully explored in order to exploit them for D2D communication.

Acknowledgment

The helpful comments by Dr. Sanket Kalamkar are gratefully acknowledged.

Appendix A
Proof of Theorem 1

Proof: Letting $\theta' = \theta r_0^{\alpha_{\rm L}}/G_{\rm m}$, we have from (5)

$$\begin{aligned}
P_{\rm s}(\theta) &= \mathbb{E}\left(\exp\left(-\theta'(I+1)/\mu\right) \mid \Phi\right)\\
&= e^{-\frac{\theta'}{\mu}} \mathbb{E} \prod_{x\in\Phi} \left(\frac{p}{1+\theta' g(\varphi_x)\ell(x)} + 1 - p\right)\\
&= e^{-\frac{\theta'}{\mu}} \prod_{i\in\{\rm L,N\}} \prod_{x\in\Phi_i} \left(\frac{p\bar{w}}{1+\theta' G_{\rm m}|x|^{-\alpha_i}} + \frac{p(1-\bar{w})}{1+\theta' G_{\rm s}|x|^{-\alpha_i}} + 1 - p\right),
\end{aligned}$$

Letting $\delta_i = 2/\alpha_i,\ i \in \{\rm L, N\}$, we have

$$\begin{aligned}
M_b &= \mathbb{E}\left[P_{\rm s}(\theta)^b\right]\\
&= e^{-\frac{b\theta'}{\mu}} \prod_{i\in\{\rm L,N\}} \mathbb{E}_{\Phi_i}\left[\prod_{x\in\Phi_i}\left(\frac{p\bar{w}}{1+\frac{\theta' G_{\rm m}}{|x|^{\alpha_i}}} + \frac{p(1-\bar{w})}{1+\frac{\theta' G_{\rm s}}{|x|^{\alpha_i}}} + 1 - p\right)^b\right]\\
&\overset{(a)}{=} e^{-\frac{b\theta'}{\mu}} \prod_{i\in\{\rm L,N\}} \exp\left(-2\pi\lambda p_i \int_0^R \left(1 - \left(\frac{p\bar{w}}{1+\frac{\theta' G_{\rm m}}{r^{\alpha_i}}} + \frac{p(1-\bar{w})}{1+\frac{\theta' G_{\rm s}}{r^{\alpha_i}}} + 1 - p\right)^b\right) r {\rm d}r\right)\\
&= e^{-\frac{b\theta'}{\mu} - \lambda\pi R^2} \exp\Bigg(\sum_{i\in\{\rm L,N\}} \lambda\pi R^2 p_i \delta_i\\
&\quad \times \int_0^1 \left(1 - \frac{p\bar{w}}{1+\frac{yR^{\alpha_i}}{\theta' G_{\rm m}}} - \frac{p(1-\bar{w})}{1+\frac{yR^{\alpha_i}}{\theta' G_{\rm s}}}\right)^b y^{\delta_i - 1} {\rm d}y\Bigg)\\
&\overset{(b)}{=} e^{-\frac{b\theta'}{\mu}} \exp\Bigg(-\sum_{i\in\{\rm L,N\}} \lambda\pi R^2 p_i \delta_i \sum_{n=1}^{\infty} \binom{b}{n} (-1)^{n+1} p^n\\
&\quad \times \sum_{m=0}^{n} \binom{n}{m} \bar{w}^m (1-\bar{w})^{n-m} \int_0^1 \frac{y^{\delta_i - 1} {\rm d}y}{\left(1+\frac{yR^{\alpha_i}}{\theta r_0^{\alpha_L}}\right)^m \left(1+\frac{yG_{\rm m}R^{\alpha_i}}{\theta r_0^{\alpha_{\rm L}} G_{\rm s}}\right)^{n-m}}\Bigg)\\
&\overset{(c)}{=} e^{-\frac{b\theta r_0^{\alpha_{\rm L}}}{G_{\rm m}\mu}} \exp\Bigg(-\sum_{i\in\{\rm L,N\}} \lambda\pi R^2 p_i \sum_{n=1}^{\infty} \binom{b}{n} (-1)^{n+1} p^n \sum_{m=0}^{n} \binom{n}{m} \bar{w}^m\\
&\quad \times (1-\bar{w})^{n-m} \tilde{F}_1\left(\delta_i, m, n-m, \delta_i+1, \frac{-R^{\alpha_i}}{\theta r_0^{\alpha_{\rm L}}}, \frac{-G_{\rm m}R^{\alpha_i}}{G_{\rm s}\theta r_0^{\alpha_{\rm L}}}\right)\Bigg),
\end{aligned}$$

where step (a) uses the probability generating functional (PGFL) of the PPP [7], step (b) follows from the general binomial theorem and step (c) is obtained with the help of the formula in [24, Eq. 3.211]. ■

Appendix B
Proof of Corollary 2

Proof: According to the proof of Theorem 1, the moment M_b is given by

$$\begin{aligned}
M_b = e^{-\frac{b\theta r_0^{\alpha_{\rm L}}}{G_{\rm m}\mu} - \lambda\pi R^2} \exp\Bigg(&\sum_{i\in\{\rm L,N\}} \lambda\pi R^2 p_i \delta_i\\
&\times \int_0^1 \left(1 - \frac{p\bar{w}}{1+\frac{yR^{\alpha_i}}{\theta r_0^{\alpha_{\rm L}}}} - \frac{p(1-\bar{w})}{1+\frac{yR^{\alpha_i} G_{\rm m}}{\theta r_0^{\alpha_{\rm L}} G_{\rm s}}}\right)^b y^{\delta_i - 1} {\rm d}y\Bigg), \quad (38)
\end{aligned}$$

where $G_{\rm m} = N$, $G_{\rm s} = 1/\sin^2\left(\frac{3\pi}{2\sqrt{N}}\right)$ and $\bar{w} = \frac{\sqrt{3}}{2\pi\sqrt{N}}$, $N > 1$. It should be noted that $N = 1$ is the omnidirectional case and thus $\bar{w} = 1$.

First of all, when $b \in \mathbb{R}^+$, we know that the term $e^{-b\theta r_0^{\alpha_{\rm L}}/(G_{\rm m}\mu) - \lambda\pi R^2}$ is monotonically increasing with N. Hence, letting $x = \frac{yR^{\alpha_i}}{\theta r_0^{\alpha_{\rm L}}}$, whether M_b is monotonically increasing with N depends on whether $\widetilde{f}(N) = \frac{\bar{w}}{1+x} + \frac{1-\bar{w}}{1+\frac{xG_{\rm m}}{G_{\rm s}}}$ is monotonically decreasing with N. In the following, we prove that $f(N) = \widetilde{f}(N^2)$ decreases monotonically, given by

$$f(N) = \frac{\sqrt{3}}{2\pi N(1+x)} + \frac{2\pi N - \sqrt{3}}{2\pi N\left(1 + xN^2\sin^2\left(\frac{3\pi}{2N}\right)\right)},\ N \geq 2, \quad (39)$$

and $f(1) = 1/(1+x)$, where $f(N)$ and $\widetilde{f}(N)$ have the same monotonicity.

Secondly, we prove $f(N)$ is monotonically decreasing with $N \geq 2$. Relaxing to $N \in [2, \infty)$, we obtain the first-order derivative of $f(N)$, given as

$$f'(N) = -\frac{\sqrt{3}}{2\pi N^2}\left(\frac{1}{1+x} - \frac{1}{1+xN^2\sin^2\left(\frac{3\pi}{2N}\right)}\right) - \frac{x(2\pi N - \sqrt{3})\sin\left(\frac{3\pi}{2N}\right)\chi(N)}{2\pi N(1+xN^2\sin^2\left(\frac{3\pi}{2N}\right))^2}, \quad (40)$$

where $\chi(N) = \sqrt{4N^2+9\pi^2}\sin\left(\frac{3\pi}{2N} - \varphi\right)$ and $\tan(\varphi) = \frac{3\pi}{2N}$. Since $N \geq 2$, we have $N^2\sin^2\left(\frac{3\pi}{2N}\right) > 1$ and $\chi(N) > 0$, thus $f'(N) < 0$ and $f(N)$ is monotonically decreasing with $N \geq 2$.

Thirdly, we can easily prove

$$f(1) - f(2) = \frac{1}{1+x} - \left(\frac{\sqrt{3}}{4\pi(1+x)} + \frac{4\pi - \sqrt{3}}{4\pi\left(1+x4\sin^2\left(\frac{3\pi}{4}\right)\right)}\right) > 0. \quad (41)$$

In summary, $f(N)$ is monotonically decreasing with N and so is $\widetilde{f}(N)$. Thus, M_b is monotonically increasing with N. When $N \to \infty$, we have $\bar{w} \to 0$, $G_{\rm m} \to \infty$ and $G_{\rm m}/G_{\rm s} \to 9\pi^2/4$. As a result, we have

$$\begin{aligned}
&\lim_{N\to\infty} M_b \\
&= e^{-\lambda\pi R^2}\exp\left(\sum_{i\in\{\rm L,N\}}\lambda\pi R^2 p_i\delta_i\int_0^1\left(1-\frac{p}{1+\frac{yR^{\alpha_i}9\pi^2}{\theta r_0^{\alpha_{\rm L}}4}}\right)^b y^{\delta_i-1}{\rm d}y\right) \\
&\overset{(a)}{=} \exp\left(-\sum_{i\in\{\rm L,N\}}\lambda\pi R^2 p_i\delta_i\sum_{n=1}^{\infty}\binom{b}{n}(-1)^{n+1}p^n\int_0^1\frac{y^{\delta_i-1}{\rm d}y}{\left(1+\frac{y9\pi^2R^{\alpha_i}}{\theta r_0^{\alpha_{\rm L}}4}\right)^n}\right) \\
&\overset{(b)}{=} \exp\Bigg(-\sum_{i\in\{\rm L,N\}}\lambda\pi R^2 p_i\sum_{n=1}^{\infty}\binom{b}{n}(-1)^{n+1}p^n \\
&\quad \times {}_2F_1\left(n,\delta_i,\delta+1,\frac{-9\pi^2R^{\alpha_i}}{4\theta r_0^{\alpha_{\rm L}}}\right)\Bigg), \quad (42)
\end{aligned}$$

where step (a) uses the general binomial theorem and step (b) follows from the definition of the Gaussian hypergeometric function in [24, Chap. 9.11]. ■

Appendix C
Proof of Theorem 3

Proof: The mean conditional local delay is given by $\mathbb{E}D_\Phi = \frac{1}{pP_{\rm s}(\theta)}$, and by averaging over Φ, the mean local delay follows as

$$\begin{aligned}
\bar{D} &= \mathbb{E}\left[\frac{1}{pP_{\rm s}(\theta)}\right] \\
&= \frac{1}{p}M_{-1}(\theta) \\
&= \frac{1}{p}\exp\left(\frac{\theta r_0^{\alpha_{\rm L}}}{G_{\rm m}\mu} - \lambda\pi R^2 + \sum_{i\in\{\rm L,N\}}\lambda\pi R^2 p_i\right. \\
&\quad \left.\times \underbrace{\delta_i\int_0^1\left(1-\frac{p\bar{w}}{1+\frac{yR^{\alpha_i}}{\theta r_0^{\alpha_{\rm L}}}} - \frac{p(1-\bar{w})}{1+\frac{yR_i^{\alpha}G_{\rm m}}{\theta r_0^{\alpha_{\rm L}}G_{\rm s}}}\right)^{-1} y^{\delta_i-1}{\rm d}y}_{A_i}\right). \quad (43)
\end{aligned}$$

Letting $v_i = \frac{R^{\alpha_i}}{\theta r_0^{\alpha_{\rm L}}}$ and $\tilde{v}_i = \frac{v_i G_{\rm m}}{G_{\rm s}}$, we have

$$\begin{aligned}
A_i &= \delta_i\int_0^1\frac{(1+v_iy)(1+\tilde{v}_iy)y^{\delta_i-1}}{(1+v_iy)(1+\tilde{v}_iy) - p(1+(\bar{w}\tilde{v}_i+(1-\bar{w})v_i)y)}{\rm d}y \\
&= 1 + \delta_i\int_0^1\frac{p(1+(\bar{w}\tilde{v}_i+(1-\bar{w})v_i)y)y^{\delta_i-1}{\rm d}y}{(1+v_iy)(1+\tilde{v}_iy) - p(1+(\bar{w}\tilde{v}_i+(1-\bar{w})v_i)y)}. \quad (44)
\end{aligned}$$

It is easy to prove that the equation of the denominator in (44) has exactly two different real roots. Denoting them by $\frac{1}{z_1}$ and $\frac{1}{z_2}$, we have

$$\begin{aligned}
A_i &= 1 + \delta_i\int_0^1\frac{p(1+(\bar{w}\tilde{v}_i+(1-\bar{w})v_i)y)y^{\delta_i-1}}{(1-z_1y)(1-z_2y)}{\rm d}y \\
&= 1 + p\tilde{F}(\delta_i,1,1,\delta_i+1,z_1,z_2) \\
&\quad + \frac{p\delta_i(\bar{w}\tilde{v}_i+(1-\bar{w})v_i)}{\delta_i+1}\tilde{F}(\delta_i+1,1,1,\delta_i+2,z_1,z_2). \quad (45)
\end{aligned}$$

Inserting (45) in (43), we obtain (33). ■

Appendix D
Proof of Theorem 4

Proof: The variance of the local delay is given as

$$\begin{aligned}
V(D) &= \mathbb{E}(D^2) - \bar{D}^2 \\
&= \mathbb{E}(\mathbb{E}(D_\Phi^2)) - \bar{D}^2 \\
&\overset{(a)}{=} \mathbb{E}\left(\frac{2-pP_s(\theta)}{(pP_s(\theta))^2}\right) - \bar{D}^2 \\
&= \frac{2}{p^2}M_{-2}(\theta) - \bar{D} - \bar{D}^2, \quad (46)
\end{aligned}$$

where step (a) follows from the second moment of the geometrically distributed random variable, and $M_{-2}(\theta)$ is given by

$$\begin{aligned}
M_{-2}(\theta) &= \mathbb{E}\left[\left(\frac{1}{P_{\rm s}(\theta)}\right)^2\right] \\
&= \exp\left(\frac{2\theta r_0^{\alpha_{\rm L}}}{G_{\rm m}\mu} - \lambda\pi R^2 + \sum_{i\in\{\rm L,N\}}\lambda\pi R^2 p_i\right. \\
&\quad \left.\times \underbrace{\delta_i\int_0^1\left(1-\frac{p\bar{w}}{1+\frac{yR^{\alpha_i}}{\theta r_0^{\alpha_{\rm L}}}} - \frac{p(1-\bar{w})}{1+\frac{yR_i^{\alpha}G_{\rm m}}{\theta r_0^{\alpha_{\rm L}}G_{\rm s}}}\right)^{-2} y^{\delta_i-1}{\rm d}y}_{B_i}\right). \quad (47)
\end{aligned}$$

Similar to the proof in the Appendix C, we have

$$\begin{aligned}
B_i &= 1 + 2(A_i-1) + \delta_i\int_0^1\frac{p^2(1+(\bar{w}\tilde{v}_i+(1-\bar{w})v_i)y)^2y^{\delta_i-1}}{(1-z_1y)^2(1-z_2y)^2}{\rm d}y \\
&= 1 + 2(A_i-1) + p^2\tilde{F}(\delta_i,2,2,\delta_i+1,z_1,z_2) \\
&\quad + \frac{2p^2\delta_i(\bar{w}\tilde{v}_i+(1-\bar{w})v_i)}{\delta_i+1}\tilde{F}(\delta_i+1,2,2,\delta_i+2,z_1,z_2) \\
&\quad + \frac{p^2\delta_i(\bar{w}\tilde{v}_i+(1-\bar{w})v_i)^2}{\delta_i+2}\tilde{F}(\delta_i+2,2,2,\delta_i+3,z_1,z_2).
\end{aligned}$$

Inserting (47) in (46), we obtain (34). ■

REFERENCES

[1] N. Deng and M. Haenggi, "The meta distribution of the SINR in mm-wave D2D networks," in *IEEE Global Communications Conference (GLOBECOM'17)*, Singapore, Dec. 2017, submitted.

[2] Z. Pi and F. Khan, "An introduction to millimeter-wave mobile broadband systems," *IEEE Communications Magazine*, vol. 49, no. 6, pp. 101–107, Jun. 2011.

[3] F. Boccardi, R. W. Heath, A. Lozano, T. L. Marzetta, and P. Popovski, "Five disruptive technology directions for 5G," *IEEE Communications Magazine*, vol. 52, no. 2, pp. 74–80, Feb. 2014.

[4] M. N. Tehrani, M. Uysal, and H. Yanikomeroglu, "Device-to-device communication in 5G cellular networks: challenges, solutions, and future directions," *IEEE Communications Magazine*, vol. 52, no. 5, pp. 86–92, May 2014.

[5] M. Haenggi, J. Andrews, F. Baccelli, O. Dousse, and M. Franceschetti, "Stochastic geometry and random graphs for the analysis and design of wireless networks," *IEEE Journal on Selected Areas in Communications*, vol. 27, no. 7, pp. 1029–1046, 2009.

[6] J. Andrews, R. Ganti, M. Haenggi, N. Jindal, and S. Weber, "A primer on spatial modeling and analysis in wireless networks," *IEEE Communications Magazine*, vol. 48, no. 11, pp. 156–163, 2010.

[7] M. Haenggi, *Stochastic geometry for wireless networks*. Cambridge University Press, 2012.

[8] T. Bai and R. W. Heath, "Coverage and rate analysis for millimeter-wave cellular networks," *IEEE Transactions on Wireless Communications*, vol. 14, no. 2, pp. 1100–1114, Feb. 2015.

[9] J. G. Andrews, T. Bai, M. N. Kulkarni, A. Alkhateeb, A. K. Gupta, and R. W. Heath, "Modeling and analyzing millimeter wave cellular systems," *IEEE Transactions on Communications*, vol. 65, no. 1, pp. 403–430, Jan. 2017.

[10] X. Yu, J. Zhang, M. Haenggi, and K. B. Letaief, "Coverage analysis for millimeter wave networks: The impact of directional antenna arrays," *accepted at IEEE Journal on Selected Areas in Communications*, 2017. [Online]. Available: https://arxiv.org/pdf/1702.04493.pdf.

[11] X. Lin, J. G. Andrews, and A. Ghosh, "Spectrum sharing for device-to-device communication in cellular networks," *IEEE Transactions on Wireless Communications*, vol. 13, no. 12, pp. 6727–6740, Dec. 2014.

[12] N. Lee, X. Lin, J. G. Andrews, and R. W. Heath, "Power control for D2D underlaid cellular networks: Modeling, algorithms, and analysis," *IEEE Journal on Selected Areas in Communications*, vol. 33, no. 1, pp. 1–13, Jan. 2015.

[13] A. Al-Hourani, S. Chandrasekharan, and S. Kandeepan, "Path loss study for millimeter wave device-to-device communications in urban environment," in *2014 IEEE International Conference on Communications (ICC) Workshop on 5G Technologies*, Jun. 2014, pp. 102–107.

[14] H. Jung and I. H. Lee, "Connectivity analysis of millimeter-wave device-to-device networks with blockage," *International Journal of Antennas and Propagation*, 2016. [Online]. Available: http://dx.doi.org/10.1155/2016/7939671.

[15] K. Venugopal, M. C. Valenti, and R. W. Heath, "Device-to-device millimeter wave communications: Interference, coverage, rate, and finite topologies," *IEEE Transactions on Wireless Communications*, vol. 15, no. 9, pp. 6175–6188, Sept. 2016.

[16] S. Wu, R. Atat, N. Mastronarde, and L. Liu, "Improving the coverage of millimeter-wave (mmwave) cellular networks using device-to-device relays," *arXiv preprint arXiv:1611.06164*, 2016.

[17] M. Haenggi, "The meta distribution of the SIR in Poisson bipolar and cellular networks," *IEEE Transactions on Wireless Communications*, vol. 15, no. 4, pp. 2577–2589, Apr. 2016.

[18] M. Salehi, A. Mohammadi, and M. Haenggi, "Analysis of D2D underlaid cellular networks: SIR meta distribution and mean local delay," *IEEE Transactions on Communications*, 2017, accepted. [Online]. Available: http://www3.nd.edu/~mhaenggi/pubs/tcom17b.pdf.

[19] Y. Wang, M. Haenggi, and Z. Tan, "The meta distribution of the SIR for cellular networks with power control," *arXiv preprint arXiv:1702.01864*, 2017.

[20] S. S. Kalamkar and M. Haenggi, "Spatial outage capacity of Poisson bipolar networks," in *2017 IEEE International Conference on Communications (ICC)*, Paris, France, May 2017.

[21] S. Singh, M. N. Kulkarni, A. Ghosh, and J. G. Andrews, "Tractable model for rate in self-backhauled millimeter wave cellular networks," *IEEE Journal on Selected Areas in Communications*, vol. 33, no. 10, pp. 2196–2211, Oct. 2015.

[22] T. S. Rappaport, G. R. MacCartney, M. K. Samimi, and S. Sun, "Wideband millimeter-wave propagation measurements and channel models for future wireless communication system design," *IEEE Transactions on Communications*, vol. 63, no. 9, pp. 3029–3056, Sept. 2015.

[23] M. Haenggi and R. K. Ganti, "Interference in large wireless networks," *Foundations and Trends in Networking*, vol. 3, no. 2, pp. 127–248, 2009.

[24] A. Jeffrey and D. Zwillinger, *Table of integrals, series, and products*. Academic Press, 2007.

[25] J. Gil-Pelaez, "Note on the inversion theorem," *Biometrika*, vol. 38, pp. 481–482, Dec. 1951.

[26] F. Baccelli and B. Blaszczyszyn, "A new phase transitions for local delays in MANETs," in *2010 Proceedings IEEE INFOCOM*, Mar. 2010, pp. 1–9.

PLACE PHOTO HERE

Na Deng received the Ph. D and B. S. degrees in electronic engineering from the University of Science and Technology of China (USTC), Hefei, China, in 2015 and 2010, respectively. From 2013 to 2014, she was a Visiting Student in Prof. Martin Haenggi's Group at the University of Notre Dame, Notre Dame, IN, USA. From June 2015 to November 2016, she was a Senior Engineer at Huawei Technologies Co., Ltd., Shanghai, China. Since then, she has been a lecturer with the School of Information and Communication Engineering, Dalian University of Technology, Dalian, China. Her scientific interests include networking and wireless communications, green communications, and network design based on wireless big data.

PLACE PHOTO HERE

Martin Haenggi (S'95-M'99-SM'04-F'14) received the Dipl.-Ing. (M.Sc.) and Dr.sc.techn. (Ph.D.) degrees in electrical engineering from the Swiss Federal Institute of Technology in Zurich (ETH) in 1995 and 1999, respectively. Currently he is the Freimann Professor of electrical engineering and a Concurrent Professor of applied and computational mathematics and statistics at the University of Notre Dame, Indiana, USA. In 2007-2008, he was a visiting professor at the University of California at San Diego, and in 2014-2015 he was an Invited Professor at EPFL, Switzerland. He is a co-author of the monograph "Interference in Large Wireless Networks" (NOW Publishers, 2009) and the author of the textbook "Stochastic Geometry for Wireless Networks" (Cambridge University Press, 2012), and he published 14 single-author journal articles. His scientific interests include networking and wireless communications, with an emphasis on cellular, amorphous, ad hoc (including D2D and M2M), cognitive, and vehicular networks. He served an Associate Editor of the Elsevier Journal of Ad Hoc Networks, the IEEE Transactions on Mobile Computing (TMC), the ACM Transactions on Sensor Networks, as a Guest Editor for the IEEE Journal on Selected Areas in Communications, the IEEE Transactions on Vehicular Technology, and the EURASIP Journal on Wireless Communications and Networking, as a Steering Committee member of the TMC, and as the Chair of the Executive Editorial Committee of the IEEE Transactions on Wireless Communications (TWC). Currently he is the Editor-in-Chief of the TWC. He also served as a Distinguished Lecturer for the IEEE Circuits and Systems Society, as a TPC Co-chair of the Communication Theory Symposium of the 2012 IEEE International Conference on Communications (ICC'12), of the 2014 International Conference on Wireless Communications and Signal Processing (WCSP'14), and the 2016 International Symposium on Wireless Personal Multimedia Communications (WPMC'16), as a General Co-chair of the 2009 International Workshop on Spatial Stochastic Models for Wireless Networks (SpaSWiN'09), and the 2012 DIMACS Workshop on Connectivity and Resilience of Large-Scale Networks, as well as a Keynote Speaker at 10 international conferences and workshops. For both his M.Sc. and Ph.D. theses, he was awarded the ETH medal, and he received a CAREER award from the U.S. National Science Foundation in 2005 and the 2010 IEEE Communications Society Best Tutorial Paper award.